HOKKAIDO UNIVERSITY

Title	Sequential layer-by-layer growth of Au nanoclusters protected by a mixed self-assembled monolayer with a polymer binding layer : Effects of pH and ionic strength of the polymer solution
Author(s)	Song, Wenbo; Okamura, Masayuki; Kondo, Toshihiro et al.
Citation	Journal of Electroanalytical Chemistry, 612(1), 105-111 https://doi.org/10.1016/j.jelechem.2007.09.017
Issue Date	2008-01-01
Doc URL	https://hdl.handle.net/2115/33006
Type	journal article
File Information	manuscript.pdf

Hokkaido University Collection of Scholarly and Academic Papers : HUSCAP

Sequential layer-by-layer growth of Au nanoclusters protected by a mixed self-assembled monolayer with a polymer binding layer - Effects of pH and ionic strength of the polymer solution

Wenbo Song,[a*] Masayuki Okamura,[b] Toshihiro Kondo[b,c] and Kohei Uosaki[b*]

[a]College of Chemistry, Jilin University, Changchun 130012, China

[b]Physical Chemistry Laboratory, Division of Chemistry, Graduate School of Science, Hokkaido University, Sapporo 060-0810, Japan

Abstract Amounts of gold nanoclusters (GNCs) in multilayer assembly with polymer binding layers has been demonstrated to be controlled by pH and ionic strength of the polymer solution when GNCs covered with mercaptoundecanoic acid (MUA) were assembled on a solid substrate in a layer-by-layer (LBL) fashion utilizing terminal carboxylate groups as charged sites to electrostatically bind to protonated amine groups of poly(allylamine hydrochloride) (PAH), which was used as a binding layer. Formation of these GNC multilayers was followed by monitoring the electrochemical response of the ferrocene moiety attached to the GNC core, which acted as a redox probe. The apparent acid dissociation constant of MUA on the GNC surface estimated from correlation between the amount of adsorbed GNCs and pH of the PAH solutions was in good agreement with those previously reported. Facile charge transport within LBL multilayer assemblies formed under various pH and/or ionic strengths of polymer solution revealed an open porous film microstructure contributing to facile charge transfer by hopping through GNC sites as well as with the aid of electrolyte in pores in such architectures. This study provides significant fundamental basis for construction of highly charged complex structures containing redox groups and useful applications in catalysis and devices fabrication based on charge transfer.

---

[*]To whom correspondence should be addressed. Tel: +81-11-706-3812, Fax: +81-11-706-3440. E-mail: uosaki@pcl.sci.hokudai.ac.jp

[c]Present address: Department of Chemistry, Faculty of Science, Ochanomizu University, Tokyo 112-8610, Japan

1. Introduction.

Assembly of nanometer-sized particles into functionalized architectures has attracted much attention because of the development of the improved nanoparticle synthesis protocols and a better understanding of their fundamental physicochemical, optical, and electronic properties as well as a wide range of potential applications in nano-scale devices [1]. Similar to classical materials and devices, the most likely implementation of nanoparticles to be used in practical applications such as sensors and opto- and electronic- devices will be in the form of thin films deposited on suitable substrates. The formation of thin films of nanoparticles is often carried out by the so-called “bottom-up wet-chemical” approach, i.e., synthesis of nanoparticles with special functionalities in solution followed by immobilization on various substrates using suitable interactions [2, 3].

Surface functionalization of inorganic nanoparticles has been accomplished during nanoparticle synthesis by adding suitable species such as organic molecules, dendrimers, and polymeric stabilizers to the reaction vessel. Colloidal routes for the synthesis of metal, e.g., Au and Ag, and semiconductor, e.g., CdS, nanoparticles bearing specific surface functionalities [4-6] are particularly attractive since surface modification can be easily achieved via covalent linkage with alkanethiol molecules having various functionalities. Such artificial molecular entities have recently been considered to be promising candidates as building blocks for nano-architectures in view of the potential applications [7].

Various wet-chemical techniques have been employed to construct multilayers of nanoparticles with surface functionalities, utilizing bond formation between a sulfur atom of an alkanedithiol, a linker, and metal atoms of a substrate as well as of a nanocluster [6,8-11], the Langmuir-Blodgett (LB) method [12,13], and electrostatic interaction between the anion and cation [14-24]. Among these, electrostatic layer-by-layer (LBL) assembly was demonstrated to be one of the most useful methods for preparing nanoparticle films with a certain degree of control over the 2D and 3D

film structures [20-24]. This method is based on an alternative adsorption of the oppositely charged polyelectrolyte and nanoparticle on solid surfaces from adsorbate solutions driven by electrostatic interactions and van der Walls force. The simplicity and versatility of the LBL method, as well as its ability of being readily amended to automation and integration with current technologies, make this technique useful for producing high quality and uniform films suitable for both fundamental and applied research. Multilayers of nanoparticles/polyelectrolytes prepared by the LBL method are robust, are permeable by solution and have low defect density, which are essential properties for many applications such as catalysis, sensing and high-density magnetic storage devices.

We have recently demonstrated the successful construction of multilayers of gold nanocluster (GNC), which were protected by mixed alkanethiol self-assembled monolayers (SAMs) containing an electrochemically active probe and a binding group, on a Au(111) surface using either copper ion or cationic polymer (poly(allylamine hydrochloride): PAH) binding layers based on the LBL principle [25-27]. GNC multilayers with thicknesses of 50-100 nm were constructed in these works and their facile formation was attributed primarily to electrostatic interactions between the carboxylate groups of MUA attached to the GNCs and amine groups of the PAH chains. The multiple charged sites of the linear PAH chain segments provide strong adhesion to the oppositely charged GNCs, and the interpenetrated polymeric nature of the whole multilayers gave the films a high degree of stability. Electrochemical investigations revealed that electrons and ions were easily transported through these multilayers [25-28].

Another advantage of the LBL procedure is that the adsorption of nanoparticles can be controlled by tailoring the surface properties of the polyelectrolyte. For example, it was demonstrated that the surface property and density of ionic functional groups in weak polyelectrolyte multilayers were strongly influenced by adsorption parameters such as pH and ionic strength [21, 29-31]. The charge density of the surfaces can be

modified by adjusting the solution pH through the protonation-deprotonation equilibrium of the amines and carboxylates groups along the polymer chains and by the addition of salt (increasing ionic strength) to the polymer solution because the potential binding sites are blocked by partial binding of ions to the charged surfaces. Based on these understandings, the adsorption parameters should be used as “tuning knobs” to modify the degree of adhesion and packing density of charged particles on the polyelectrolyte film surface via shielding and secondary interactions.

Here we investigated in detail the effects of the adsorption parameters of LBL adsorbate solutions, pH and ionic strength, on the GNC adsorption density to provide a protocol of the ideal LBL approach for multilayer assembly of nanoparticles interlaced with polymer layers. Principles of the incorporation of charged GNC into LBL multilayers were clarified in this study. Charge transfer mechanism in these LBL multilayer assemblies formed in polymer solutions of various pH and/or ionic strengths were discussed. Novelties of the work are the tunable microstructures and their facile charge transport in these architectures. Controllable uptake of functional adsorbents and facile charge transfer in the assembly are essential to fabrication of sensor and device based on charged transport by considering the sensitivity and other properties. This work represents a very useful controlled test-bed for fundamental studies on incorporation of redox groups in highly charged film and paves a way to practical device and sensor applications based on charge transfer.

2 Experimental

2.1 Materials

Poly(allylamine hydrochloride) (PAH) (average Mw = 70,000) was purchased from Aldrich Chem. Co. Perchloric acid (ultrapure grade), sodium chloride and sulfuric acid (ultrapure grade) were obtained from Wako Pure Chemicals. All chemicals were used as received. Tin-doped indium oxide (ITO) thin film-coated glass was obtained from

Tokyo Kinoene Optics. Ultrapure water was obtained using a Milli-Q water purification system (Millipore), and ultrapure N_2 (99.999 %) was obtained from Air Water.

2.2 Preparation of GNCs covered with SAMs

GNC covered by mixed SAMs of hexanethiol (C_6SH), ferrocenylhexanethiol (FcC_6SH), and mercaptoundecanoic acid (MUA) used in this work was prepared by a combination of the modified Schiffrin's and the place-exchange methods. Briefly, a C_6SH SAM-protected gold nanocluster was prepared by the two-phase synthesizing method reported by Brust et al. [4]. Then FcC_6SH and MUA were introduced sequentially onto the surface of C_6SH SAM-protected GNC by the place-exchange method [32]. The preparation of the GNC was described in detail in our earlier reports [25-28]. The resultant GNC has a core diameter of 1.8 ± 0.4 nm, which was determined by transmission electron microscopy (TEM, JEOL-2000EX, 200 kV). The molar ratio of C_6SH : FcC_6SH : MUA on the GNC surface estimated by ^{1}H-NMR (Hitachi, R-1900, 90 MHz) was 47: 19: 34.

2.3 LBL growth of GNC multilayers

A multilayer of MHF-GNC was constructed on an ITO substrate with an apparent surface area of 1 cm^2 based on carboxylate/polycation electrostatic interaction. The ITO substrate was cleaned by immersing in a 1:3 H_2O_2 (30%)- H_2SO_4 (conc.) solution for 5 s, rinsed thoroughly with Milli-Q water, and finally dried with ultrapure nitrogen. The cleaned ITO substrate was immediately transferred to an ethanol solution containing 1 mM MUA and kept in the solution for at least 36 h. After the ITO substrate had been thoroughly rinsed with ethanol and dried by blowing ultrapure nitrogen, a GNC multilayer was constructed by alternately dipping the ITO substrate in 2.0 mg/ml PAH aqueous solution followed by a rinse with an aqueous solution of the same pH of the

PAH solution and in 1.0 mg/ml GNC ethanol solution followed by a rinse with ethanol. Both PAH and GNC were found to be adsorbed quickly and the dipping period was 10 min in each solution, which was determined from the time when the charge due to the ferrocene redox in the cyclic voltammogram (CV) of the multilayers became constant. Because the addition of salt and acid/basic solution may lower the solubility of GNCs covered with SAMs, leading to aggregation and/or precipitation of GNCs, due to the charge shielding effect, adjustment of pH and ionic strength was carried out only in the PAH solution. Multilayers of GNC were constructed on ITO surfaces by systematically varying the pH of PAH dipping solution from 2.5 to 8.0. The pH of the polymer solution was adjusted to the desired value by adding 0.2 M NaOH and HCl solutions, and ionic strength of the PAH solution was modulated by adding NaCl. To study the effect of pH on the GNC growth, a fixed amount of NaCl (0.5 M) was added to the PAH solution to keep the ionic strength constant, which should effectively eliminate the interference of the salt effect caused by the addition of a base and acid used to adjust the solution pH. For the salt concentration-dependent GNC deposition experiment, the pH of the polymer solution was controlled to be ca. 6. After each deposition cycle (two dipping and rinsing steps) had been completed, the ITO substrate was dried by blowing ultrapure nitrogen and electrochemical measurement was carried out.

2.4 Characterization

Cyclic voltammograms (CVs) were obtained in a 0.1 M $HClO_4$ aqueous solution, which was thoroughly deaerated by passing ultrapure nitrogen gas through it for more than 30 min before each measurement using an HSV-100 automatic polarization system (Hokuto Denko). A Pt wire and a Ag/AgCl electrode were used as a counter and a reference electrode, respectively.

3. Results and Discussion

3.1 Effect of pH on the LBL growth of GNC/PAH multilayers

Figure 1 shows the CVs of the GNC/PAH multilayers in a PAH aqueous solution of pH 6 with 0.5 M NaCl at various deposition cycles measured in a 0.1 M $HClO_4$ aqueous solution at a scan rate of 100 mV s^{-1}. Quasi-reversible current peaks due to redox of the ferrocene moieties in the multilayers were observed at around 350 mV (vs. Ag/AgCl) for all the samples. The charge corresponding to the anodic peak linearly increased with increase in the number of deposition cycles, indicating uniform accumulation of ferrocene (Fc) groups, i.e., incorporation of the GNCs, by each deposition cycle.

Electrochemical behaviors of the GNC multilayers assembled under other pH conditions showed a tendency similar to that of the GNC multilayers formed at pH 6. Figure 2 shows the pH dependence of the anodic charge of GNC at various deposition cycles. The charge depended on both the GNC deposition cycle and the pH of the PAH solution. At a given deposition cycle, the charge initially increased slightly with increase of pH from 2.5 to 5.0, then greatly increased as the pH was increased further from 5.0 to 7.0, and finally reached saturation when pH became 8.0. At a given pH, the charge increased with increase in the number of deposition cycles as shown in Figure 3, in which anodic charges are plotted against the number of deposition cycles at various pH. The increase in charge by two successive deposition cycles at higher pH (pH>6) was much more pronounced than that at lower pH (pH<5). The average increment of the charge per deposition cycle obtained from the slope of the charge – deposition cycle relation is plotted as a function of PAH solution pH in the inset of Figure 3.

The pH dependence of the amounts of polymers in alternate-layered films, which are composed of polycations, e.g., protonated amines, and polyanions, e.g., carboxylates, has been described as "titration" of one polyelectrolyte by the other based on the protonation-deprotonation equilibrium [29-31]. A similar picture should apply to the GNC/PAH films described in this paper, and the multilayer formation is expected to be

governed by the acid-base chemistry at the interface through tuning of the pH of PAH solution during the LBL growth. Since PAH is a polyelectrolyte of weak base, the pKa of which is 9 - 11 in an aqueous solution [33], the PAH chains were fully ionized with positive charge in all of the PAH solutions used in this study, the pH values of which were between 2.5 and 8.0. On the other hand, the charge of the SAM-covered GNC at the PAH-covered ITO substrate should depend on the pH of the PAH solution used for the multilayer formation because pKa of MUA was around 6 [34-36].

When a PAH layer was deposited on an MUA-covered ITO substrate from a PAH solution with pH between 2.5 and 8.0, fully charged polymer chains should be deposited on the ITO surface. When the ITO surface with a PAH layer was exposed to the GNC solution, the acid/base property should be retained at the interface [19] and the state of protonation of the incoming GNCs at the interface was controlled by the acid/base property of the ITO surface because no attempt was made to buffer the GNC dipping solution. Thus, when the GNC/PAH multilayers were formed at low pH such as 2.5, the retained interfacial acidity was not favorable for ionization of the MUA group on the incoming GNCs, resulting in GNCs having either completely neutral or very low negative surface charge. As a result, no or very weak electrostatic interaction was expected between the PAH-modified ITO surface and the GNCs, leading to a small amount of GNC adsorption on the PAH-modified ITO surface. In this particular case, hydrogen bonding might play an important role in the LBL multilayer formation. As the pH of PAH solution became higher, the retained interfacial acidity of the polymer layer became lower, resulting in more ionized carboxylate groups on the incoming GNC surfaces and stronger electrostatic interaction between the PAH-modified ITO surface and the GNCs, leading to adsorption of a larger amount of GNCs on the PAH-modified ITO surface. When the pH of PAH solution became high enough, all of the carboxylate groups on the incoming GNC surfaces were ionized and the electrostatic interaction between the PAH-modified ITO surface and the GNCs as well as the amount of the adsorbed GNCs on the PAH-modified ITO surface reached maximum, i.e., saturated,

values. Thus, the shape of the curves in Fig. 2 and more accurately that of the curve in the inset of Fig. 3 should reflect the dissociation behavior of carboxylic acid of MUA on the GNCs. Thus, the apparent acid dissociation constant of MUA attached to the GNC surface, interfacial pKa, can be determined as the pH at half total charge change in the inset of Fig. 3, i.e., 5.8. Shimazu et al. reported the surface pKa values of MUA in both homogeneous SAM and mixed SAMs with alkanethiol to be 4.8 and 5.6, respectively, as determined by the surface mass titration method using a quartz crystal microbalance and showed that the pKa values became smaller with increase in the repulsive interaction between carboxylates in SAMs [34-36]. The pKa value of 5.8 found for MUA on the GNCs is in good agreement with the value of 5.6 reported for the mixed SAMs, confirming that the amount of deposited GNCs is controlled by the pH-dependent dissociation behavior of carboxylic acid of MUA on the GNCs.

Electrochemical parameters obtained from CVs are summarized in Table 1. Although the anodic and cathodic peak potentials shifted in positive and negative directions, respectively, and, therefore, the peak separation increased as the pH of the PAH solution or the number of deposition cycles increased, the formal potential of the redox of the Fc moiety ($(Ep_a + Ep_c)/2$) was almost constant at around 350 mV independent of the pH of PAH solution and the number of deposition cycles. Peak separation at a given deposition cycle was larger when the GNC multilayer was formed in a PAH solution of higher pH. For example, peak separations at the ITO electrodes modified with GNC/PAH multilayers with ten deposition cycles were 45, 46, 56, 73, 120 and 123 mV at pH values of 2.5, 4.0, 5.0, 6.0, 7.0 and 8.0, respectively.

Figure 4 shows the relation between the peak separation (Table 1) and anodic charge (Fig. 2) of the Fc redox peak, i.e., the amount of GNCs, of the GNC multilayers prepared in PAH solutions of various pH. The peak separation increased almost linearly with the charge but was hardly dependent on pH at a given charge. Fluctuations in data are likely due to the disordered architecture of the film driven by the nature of the self-assembly process. Thus, although the amount of deposited GNC was controlled by

pH and number of deposition cycles, the peak separation was dependent only on the amount of deposited GNC. Since larger peak separation shows slower electron transfer kinetics, the progressive increase in peak separation with increase in the amount of deposited GNC/PAH layer suggests that the GNC/PAH multilayers formed on the ITO surface became denser and thicker, resulting in more kinetically hindered charge transfer through these films, as a larger amount of the GNC/PAH layers were deposited. The constant peak separation at a given charge regardless of the pH of PAH solution shows that the quality of the multilayer was not affected by the pH of PAH solution.

Information about the role of film structure on charge transfer within the film can also be obtained from the full width of half maximum (fwhm) of the Fc redox peak (denoted briefly as $W_{1/2}$) given in Table 1. The peak was found to be gradually broadened with increase in the GNC/PAH deposition cycle at all pH values and the pH of the PAH solution. Observed increases in peak width in different multilayers suggest that Fc molecules likely reside in different microenvironments and also point to a disordered, inhomogeneous film structure. $W_{1/2}$ of the Fc redox peak varied in the range of 40-90 mV, which were much smaller than those in the Fc-functionalized dithiol-gold nanoparticle LBL films [24], suggesting relatively strong attractive interaction between ferrocene groups [37, 38].

3.2 Effect of ionic strength on the LBL growth of GNC/PAH multilayers

The effect of ionic strength on multilayer assembly of GNCs was examined using a PAH solution of pH=6. Well-defined redox peaks were observed at ca. 350 mV (vs. Ag/AgCl) in all cases. Electrochemical parameters obtained from CVs are summarized in Table 2. The peak separation was increased from ca. 20 mV (for N=1 at all salt concentrations) to 138 mV (N=10 at 2.0 M NaCl). Peak separation depended on both the deposition cycle and the ionic strength. The half-width of the Fc oxidation peak was

less than 90 mV in almost all cases, implying a closely packed arrangement of GNCs in these multilayers as discussed before.

Figure 5 shows the anodic charges of the Fc moiety in these GNC multilayers as a function of the deposition cycle. The charges increased almost linearly with increase in the number of deposition cycles up to 10 cycles in all cases, indicating uniform layer growth. The average amount of adsorbed GNCs at each deposition cycle at a given salt concentration of the PAH solution, i.e., the slope of linear relations in Figure 5, was dependent on salt concentration as shown in Figure 6. Multilayers with relatively small amounts of GNC adsorption were achieved in a salt-free PAH solution. The adsorption amount increased greatly with the addition of a small amount of NaCl and increased further but slightly with increase in salt concentration. It is interesting to note that multilayer films could be formed even if the NaCl concentration was as high as 2 M. This behavior is in contrast to that of the adsorption of weak polyelectrolyte, which tends to desorb under high ionic strength conditions [39].

The present results suggest that other hydrophobic interactions between the hexanethiolate part of the GNC monolayers and the polymer play a role in the adsorption process. A possible reason for the increases of GNC adsorption with addition of salt to the PAH solution is the ionic strength dependent conformation of PAH. In a salt-free polymer solution, PAH should be in a rather extended conformation and adsorbed at the surface like a flat pancake due to the repulsive interactions between the charged sites along the polymeric chains. The GNC anions adsorbed primarily at the top of the PAH interface in this case. The conformation of the adsorbed polyelectrolyte is expected to change to a more condensed, coiled conformation as ionic strength was increased because of the effective shielding of the surface charge [40]. Thus, the adsorbed amount of PAH per unit area is expected to be large when ionic strength is high and GNCs not only adsorbed on top of the PAH interface but also diffused into the PAH layer, binding to internal sites of PAH through ion exchange of uncompensated anions, resulting in higher amount of GNCs within these multilayers.

4. Conclusions

GNC covered with mixed SAMs consisting of both an electro-active probe, Fc, and a binding group, MUA, was used as a building block to construct multilayers on a solid surface with a cationic polymer, PAH, based on the layer-by-layer assembling principle under the conditions of various pH and salt concentrations. The adsorption density of GNCs in the multilayers was demonstrated to be controlled through variation of pH and ionic strength of the PAH solution. The apparent acid dissociation constant of MUA, pKa, on the GNC surface estimated from the pH-dependent sequential LBL growth of GNC, was in good agreement with those previously reported. Small peak separation of redox of Fc moieties in all LBL multilayer assemblies formed in polymer solutions of various pH and/or ionic strengths revealed a facile charge transport microstructures in all such architectures. Both nanostructured building blocks and open porous film microstructure imply key roles in facile charge transfer by hopping through GNC sites as well as with the aid of electrolyte in pores in such architectures. This study provides not only significant fundamental basis for construction of complex structures and devices containing charged meso-scale objects and biomacromolecules but also very useful implications in catalysis and sensors and devices fabrication based on charge transfer.

Acknowledgements

WS acknowledges the National Natural Science Foundation of China (Grant No. 20543003) and the Japan Society for the Promotion of Science for a Postroctoral Fellowship for Foreign Scientists. This work was partially supported by a Grant-in-Aid for Scientific Research (KAKENHI) in Priority Area of "Molecular Nano Dynamics" (Nos. 16072202 and 17034017) from the Ministry of Education, Culture, Sports,

Science and Technology. We thank Dr. Sugawara for his help with the TEM measurement.

References

[1] G. Schmid, Clusters and Colloids, VCH, Weinheim, 1994.

[2] J. H. Fendler, Chem. Mater., 8 (1996) 1616.

[3] A. N. Shipway, E. Katz, I. Willner, Chem. Phys. Chem. 1 (2000) 18.

[4] M. Brust, M. Walker, D. Bethell, D. J. Schiffrin, R. J. Whyman, Chem. Soc. Chem. Commun. (1994) 801.

[5] M. D. Malinsky, K. L. Kelly, G. C. Schatz, R. P. Van Duyne, J. Am. Chem. Soc. 123 (2001) 1471.

[6] V. L. Colvin, N. Goldstein, A. P. Alivasatos, J. Am. Chem. Soc. 114 (1992) 5221.

[7] A. C. Templeton, W. P. Wuelfing, R. W. Murray, Acc. Chem. Res. 33 (2000) 27 and references therein.

[8] S. Chen, R. W. Murray, S. W. Feldberg, J. Phys. Chem. B 102 (1998) 9898.

[9] S. Ogawa, F.-R. Fan, A. J. Bard, J. Phys. Chem. 99 (1995) 11182.

[10] T. Nakanishi, B. Ohtani, K. Uosaki, J. Phys. Chem. B 102 (1998) 1571.

[11] H. Inoue, N. Ichiroku, T. Torimoto, T. Sakata, H. Mori, H. Yoneyama, Langmuir 10 (1994) 4517.

[12] T. Torimoto, N. Tsukasa, H. Nakamura, S. Kuwabata, T. Sakata, H. Mori, H. Yoneyama, Electrochim. Acta 45 (2000) 3269.

[13] T. Torimoto, N. Tsumura, M. Miyake, M. Nishizawa, T. Sakata, H. Mori, H. Yoneyama, Langmuir 15 (1999) 1853.

[14] J. Schmitt, G. Dcher, W. J. Dressick, S. L. Brandow, R. E. Geer, R. E. Shashidhar, J. M. Calvert, Adv. Mater. 9 (1997) 61.

[15] F. P. Zamborini, J. F. Hicks, R. W. Murray, J. Am. Chem. Soc. 116 (2000) 4514.

[16] A. C. Templeton, F. P. Zamborini, W. P. Wuelfing, R. W. Murray, Langmuir 16 (2000) 6682.

[17] A. C. Templeton, W. P. Wuelfing, R. W. Murray, Acc. Chem. Res. 33 (2000) 27.

[18] J. F. Hicks, Z. P. Zamborini, A. Osisek, R. W. Murray, J. Am. Chem. Soc. 123 (2001) 7048.

[19] J. F. Hicks, Y. Seok-Shon, R. W. Murray, Langmuir 18 (2002) 2288.

[20] K. M. Chen, X. Jiang, L. C. Kimerling, P. T. Hammond, Langmuir 16 (2000) 7825.

[21] M. E. Tagliazucchi, E. J. Calvo, J. Electroanal. Chem. 599 (2007) 249.

[22] M. T. Crisp, N. A. Kotov, Nano. Lett. 3 (2003) 173.

[23] M. Chirea, V. García-Morales, J. A. Manzanares, C. Pereira, R. Gulaboski, F. Silva, J. Phys. Chem. B 109 (2006) 21808.

[24] A. Escorcia, Al-Amin Dhirani, J. Electroanal. Chem. 601 (2007) 260.

[25] T. Kondo, M. Okamura, K. Uosaki, Chem. Lett. (2001) 930.

[26] K. Uosaki, T. Kondo, M. Okamra, W. Song, Faraday Discuss. 121 (2002) 373.

[27] W. Song, M. Okamura, T. Kondo, K. Uosaki, J. Electroanal. Chem. 554-555 (2003) 385.

[28] W. Song, M. Okamura, T. Kondo, K. Uosaki, Phys. Chem. Chem. Phys. 5 (2003) 5279.

[29] S. Shiratori, M. F. Rubner, Macromolecules 33 (2000) 4213.

[30] D. Yoo, S. S. Shiratori, M. F. Rubner, Macromolecules 31 (1998) 4309.

[31] G. Decher, Science 277 (1997) 1232.

[32] M. J. Hostetler, A. C. Templeton, R. W. Murray, Langmuir 15 (1999) 3782.

[33] O. Mermut, C. J. Barret, J. Phys. Chem. B 107 (2003) 2525.

[34] K. Shimazu, T. Teranishi, K. Sugihara, K. Uosaki, Chem. Lett. (1998) 669.

[35] K. Sugihara, T. Teranishi, K. Shimazu, K. Uosaki, Electrochemistry 67 (1999) 1172.

[36] K. Sugihara, K. Shimazu, Langmuir 16 (2000) 7101.

[37] K. Uosaki, Y. Sato, H. Kita, Langmuir 7 (1991) 1510.

[38] K. Uosaki, Y. Sato, H. Kita, Electrochim. Acta 36 (1991) 1799.

[39] G. Decher, J. D. Hong, J. Schumitt, Thin Solid Films 210-211 (1992) 831.

[40] W. Knoll, Curr. Opin. Colloid Interface Sci. 1 (1996) 137.

Table 1. Effects of pH of PAH solution and number of deposition cycles, N, on anodic, E_{pa}, and cathodic, E_{pc}, peak potentials, formal potential, E_0, and full width of half maximum of anodic peak, $W_{1/2}$, corresponding to the redox of the ferrocene group of GNC multilayers.

pH	2.5				4				5				6				7				8			
N	E_{pa}	E_{pc}	E_0	$W_{1/2}$	E_{pa}	E_{pc}	E_0	$W_{1/2}$	E_{pa}	E_{pc}	E_0	$W_{1/2}$	E_{pa}	E_{pc}	E_0	$W_{1/2}$	E_{pa}	E_{pc}	E_0	$W_{1/2}$	E_{pa}	E_{pc}	E_0	$W_{1/2}$
1	362	342	352	45	360	344	352	46	360	344	352	46	356	340	348	47	360	340	350	47	359	341	350	47
2	370	340	355	50	365	335	350	44	365	332	349	59	363	335	349	49	370	333	352	48	367	332	350	47
3	370	338	354	58	364	332	349	43	366	335	351	49	364	335	350	56	373	327	352	56	374	323	348	49
4	370	333	352	67	370	333	352	47	368	330	349	65	372	327	350	51	382	324	253	58	382	320	351	72
5	370	335	353	72	370	332	351	66	373	332	353	67	375	327	352	69	385	323	354	73	384	320	352	77
6	372	332	352	70	370	330	350	60	375	328	352	68	379	330	355	70	387	312	350	69	390	312	351	72
7	373	330	352	80	373	332	353	57	376	324	348	72	380	326	353	73	400	304	352	72	396	310	353	86
8	370	332	351	83	380	323	352	67	382	323	353	77	387	324	355	83	403	302	353	73	400	304	352	90
9	375	330	353	85	377	330	354	60	378	330	354	80	389	319	354	80	404	300	352	75	404	300	352	90
10	375	330	353	80	376	330	353	70	378	322	350	80	389	316	356	78	415	295	355	80	413	290	352	88

Table 2. Effects of salt concentration, C_{salt}, of PAH solution of pH = 6 and number of deposition cycles, N, on peak separation, ΔE_p, of anodic and cathodic peak potentials and full width of half maximum of anodic peak, $W_{1/2}$, corresponding to the redox of the ferrocene group of GNC multilayers.

C_{salt} (M)	0		0.25		0.50		0.75		1.0		1.5		2.0	
N	ΔE_p	$W_{1/2}$	ΔE_p	$W_{1/2}$	ΔE_p	$W_{1/2}$	ΔE_p	$W_{1/2}$	ΔE_p	$W_{1/2}$	ΔE_p	$W_{1/2}$	ΔE_p	$W_{1/2}$
1	15	45	18	45	18	45	18	48	20	50	20	50	22	53
3	28	50	45	48	47	48	50	50	50	50	50	52	50	56
5	45	51	52	52	65	53	65	58	72	62	60	60	70	78
8	52	73	82	77	85	84	90	88	100	92	95	85	110	95
10	60	88	110	91	95	90	95	92	110	98	110	90	138	97

Figure Captions

Figure 1 Cyclic voltammograms of the LBL sequential adsorption of GNC/PAH binding layers in a PAH solution of pH 6 containing 0.5 M NaCl measured in a 0.1 M $HClO_4$ aqueous solution at a scan rate of 100 mV s^{-1}. The number of GNC deposition cycles is shown in the figure.

Figure 2 Variation of electronic charge corresponding to the anodic peak of the ferrocene group during the sequential deposition of GNC on ITO electrodes in the pH range of 2.5 to 8.0. The number of GNC deposition cycles is described in the figure.

Figure 3 Anodic charge corresponding to the redox of the ferrocene group as a function of deposition cycle at various pH. Inset: pH dependence of an increment of charge at each deposition cycle, i.e., slope of the charge - deposition cycle relation.

Figure 4 Correlations of peak separation of the Fc group with the anodic charge of the Fc redox peak during sequential LBL growth of GNC multilayers at various pH.

Figure 5 Electronic charges corresponding to the anodic peak of the ferrocene group of the GNC multilayers constructed PAH solutions of various salt concentrations as a function of GNC deposition cycle. Salt (NaCl) concentration is shown in the figure.

Figure 6 Increment in anodic charge of the ferrocene moiety of GNC multilayers formed in PAH solutions of various salt (NaCl) concentrations.

Figure 1

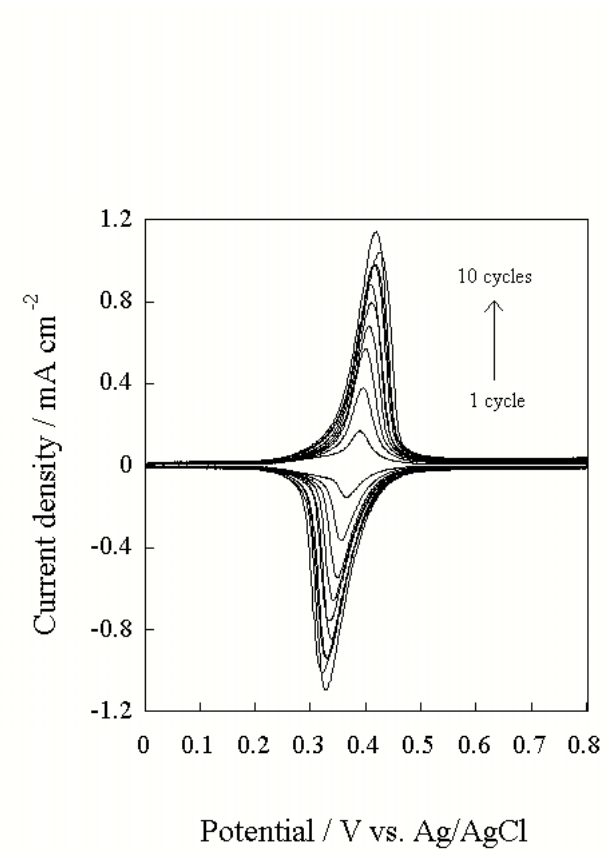

1.2
0.8
0.4
0
-0.4
-0.8
-1.2
0
0.1
0.2
0.3
0.4
0.5
0.6
0.7
0.8
10 cycles
1 cycle
Current density / mA cm-2
Potential / V vs. Ag/AgCl

Figure 2

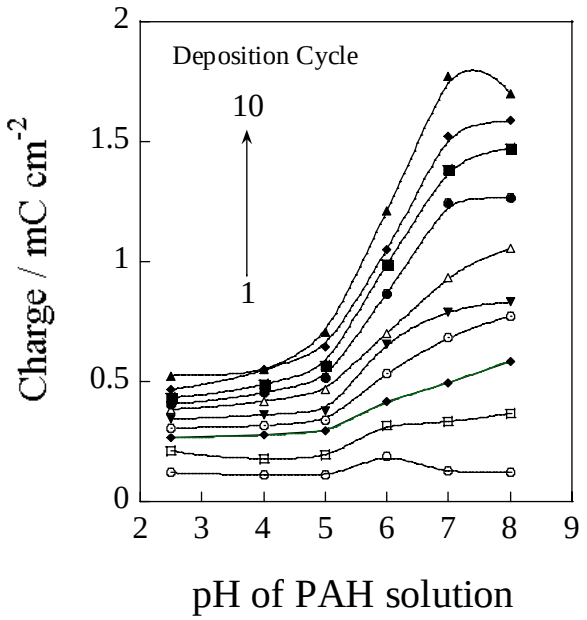

Deposition Cycle
10
1
Charge / mC cm-2
pH of PAH solution
0
0.5
1
1.5
2
2
3
4
5
6
7
8
9

Figure 3

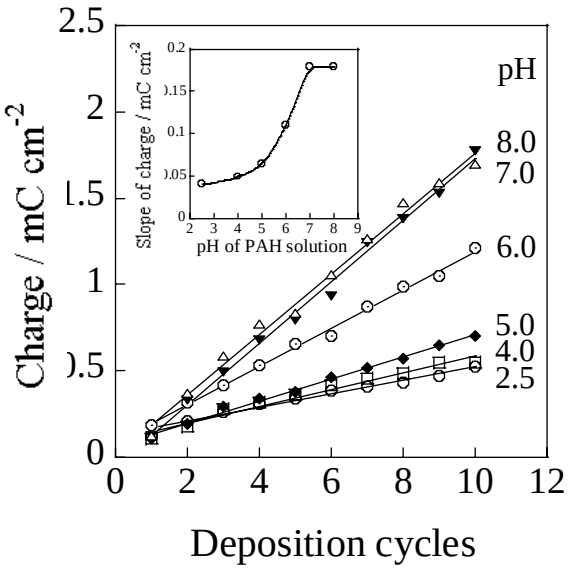

Charge / mC cm-2
Deposition cycles
pH
8.0
7.0
6.0
5.0
4.0
2.5
Slope of charge / mC cm-2
pH of PAH solution

Figure 4

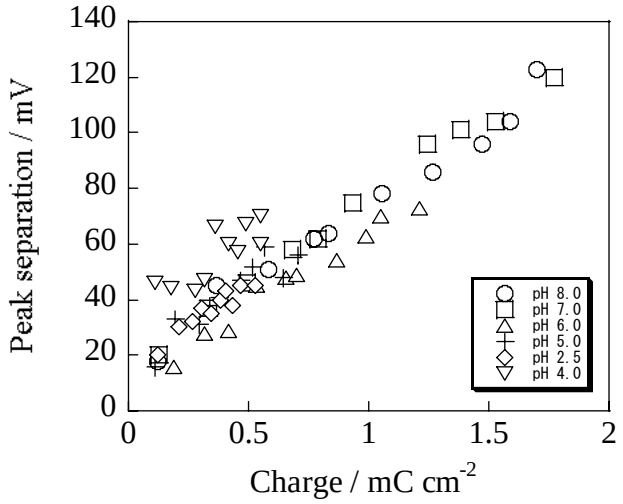

Peak separation / mV
Charge / mC cm-2
0
20
40
60
80
100
120
140
0
0.5
1
1.5
2
pH 8.0
pH 7.0
pH 6.0
pH 5.0
pH 2.5
pH 4.0

Figure 5

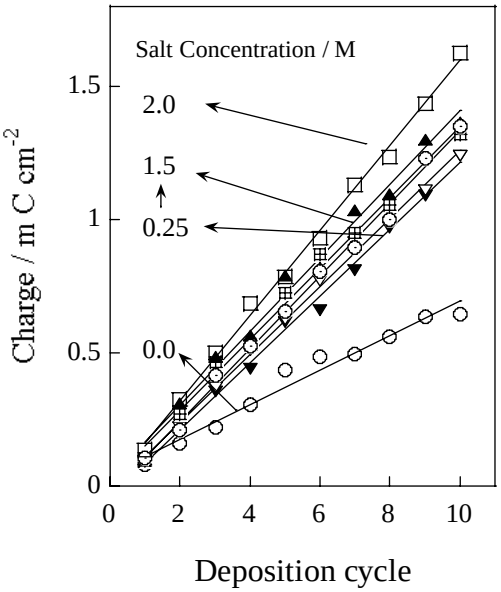
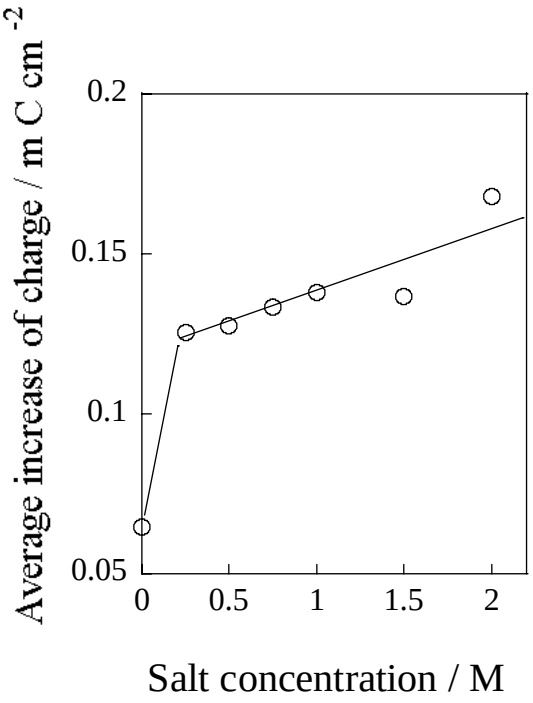

Salt Concentration / M
2.0
1.5
0.25
0.0
Charge / m C cm-2
Deposition cycle
0
0.5
1
1.5
0
2
4
6
8
10

Figure 6


Average increase of charge / m C cm -2
0.2
0.15
0.1
0.05
0
0.5
1
1.5
2
Salt concentration / M